J. Physiol. (1981), **318**, *pp.* 279–295
With 7 text-figures
Printed in Great Britain

SIMULTANEOUS CHANGES IN THE EQUILIBRIUM POTENTIAL AND POTASSIUM CONDUCTANCE IN VOLTAGE CLAMPED RANVIER NODE IN THE FROG

BY J. M. DUBOIS

From the Laboratoire de Neurobiologie, Ecole Normale Supérieure 46, rue d'Ulm, 75230 Paris Cedex 05, France

(*Received 6 August 1980*)

SUMMARY

1. In voltage clamped myelinated nerve fibres, the K^+ conductance has been calculated from current recordings obtained in low and high K^+ media, taking into account the changes in E_K resulting from accumulation or depletion of K^+ ions near the nodal membrane.

2. At the end of a depolarization, the instantaneous K^+ current reverses at a potential (instantaneous reversal potential) differing from the Nernst potential calculated using the external and internal bulk concentrations (theoretical Nernst potential). During a depolarization, E_K, as estimated from the instantaneous reversal potential, changes continuously. This change depends on the size, the duration and the direction of the time dependent K^+ current. The variation of E_K is attributed to continuous changes in K^+ concentration near the membrane during voltage pulses which turn on the K^+ conductance.

3. The chord conductance $[G_K = I_K/(E-E_K)]$, as calculated using the instantaneous reversal potential values for E_K, has been analysed as a function of time and membrane potential. As previously reported it increases with the initial K^+ concentration in the external medium.

4. The time course of the K^+ current depends on both the kinetics of the conductance increase and the rate of change in the driving force for K. The kinetics of the conductance increase can satisfactorily be described by a single exponential function following a delay after the onset of the depolarizing voltage clamp pulse.

5. This delay increases when the holding potential is made more negative. It decreases with membrane depolarization and it is independent of the external K^+ concentration. At a given membrane potential, the turning on of the K^+ conductance is found to be faster at high than at low external K^+ concentrations.

6. At repolarization, the turning off of the conductance cannot be described by a single exponential function. It is faster at low than at high external K^+ concentrations.

7. The results suggest that the change in K^+ conductance proceeds in a multi-step transition or (and) that the K^+ conductance is determined by several types of K^+ channels.

INTRODUCTION

In the Hodgkin–Huxley formalism, the kinetics of the activation of the K^+ system in the nodal membrane are described by: $P_K = \overline{P}_K n^a$, where P_K is the permeability coefficient as calculated (Frankenhaeuser, 1962) on the basis of the constant field equation (Goldman, 1943; Hodgkin & Katz, 1949), $\overline{P}_K$ is the maximum permeability and n^a is the fraction of channels open. In this expression, the exponent a reflects the number of membrane subunits necessarily cooperating to open the channel when the membrane is depolarized. Various values for a (at the node of Ranvier) have been proposed, including 2 (Frankenhaeuser, 1963) and 4 (Dodge, 1963; Koppenhöfer, 1967; Hille, 1968). Moreover, hyperpolarizing conditioning pulses delay the onset of K^+ current (Palti, Ganot & Stämpfli, 1976; Ganot, Palti & Stämpfli, 1978; Begenisich, 1979). This phenomenon, first described in the squid axon (Cole & Moore, 1960) can be accounted for by the two-state Hodgkin–Huxley model by increasing the value of a. However, this raises serious difficulties for interpreting in physical terms the molecular events underlying the changes in permeability. Alternatively, it can be accounted for according to three interpretations: (i) the K^+ conductance is determined by a multi-state process; (ii) the K^+ conductance is determined by two or more types of K^+ channels; (iii) the K^+ current is affected by some extra axonal parameters (Ganot *et al.* 1978). In this paper and the following (Dubois, 1981), several arguments are presented which support these interpretations. The third interpretation can be supported by the observation of a change in driving force due to accumulation of K^+ ions in the perinodal space during a depolarizing voltage pulse (Dubois & Bergman, 1975*b*). Such a phenomenon has already been described by Frankenhaeuser & Hodgkin (1956) and Adelman, Palti & Senft (1973) for the squid giant axon.

This paper confirms the existence of marked variations in the equilibrium potential for K^+ ions (E_K), at the node of Ranvier, during membrane depolarizations. A kinetic analysis of the potassium currents has been performed and corrections for the changes in E_K have been taken into account to calculate the actual time course of the conductance increase.

METHODS

The experiments were done on voltage clamped motor and sensory myelinated fibres from the sciatic nerve of the frog *Rana esculenta*. The membrane currents were recorded using the method of Nonner (1969). The two ends of the fibre were cut and kept in isotonic (117 mM) KCl solution filling the two side pools of the chamber. Assuming 117 mM for the bulk axoplasmic K^+ concentration, 15–20 min after the fibres were cut (Palti, Gold & Stämpfli, 1979) the zero potential was determined as the reversal potential for the steady-state K^+ current in 117 mM-K solution. The holding potential ($E = -90$ mV) was the same in all experiments. Membrane currents were measured as a voltage drop across the axoplasmic resistance estimated to be 10 MΩ. Leakage and capacity currents, assumed proportional to the voltage change, were automatically subtracted from the total membrane current by means of an analog compensation previously described (Dubois & Bergman, 1977). The resulting signal was filtered (R–C filter; cut-off frequency: 30 kHz or 10 kHz). The accuracy of the compensation was tested from leakage and capacity current responses to large hyperpolarizing pulses throughout the whole experiment and before each voltage clamp run. An example of such a compensation is given in Fig. 1*A*. In some cases, the records were averaged by means of a signal averager (time resolution: 20 μsec). The use of this method is based on the assumption that the time independent current (leakage current) and the capacity current are linear over all the potential range studied. The capacity transient will, in fact, not be perfectly linear because of the gating current activated at positive membrane potentials. At large positive membrane potentials, the gating current is less than 10 % of the total capacity current. Dubois & Bergman (1975*a*) and Attwell, Dubois & Ojeda (1980) found in the presence of TEA and TTX that the time independent current is approximately, but not, perfectly linear. These approximations will introduce some error in the currents measured.

Solutions

The node was superfused with Ringer or test solutions at constant temperature (12 °C). The Ringer solution had the following composition (mM) NaCl: 111·5; KCl: 2·5; $CaCl_2$: 1·8; $NaHCO_3$: 2·4; pH: 7·4. The test solutions were modifications of the Ringer solution. In these solutions, part or all of the Na^+ was replaced by K^+. 10^{-6} M-tetrodotoxin was added to all solutions to block the sodium current.

Nomenclature

The absolute membrane potential (E) is defined as internal potential minus external. Accordingly, negative currents are inward.

Much of the work in this paper is based upon measurements of the reversal potential for instantaneous K^+ currents. This potential is referred to as the '*instantaneous reversal potential*' and is regarded as the actual equilibrium potential for K^+ ions at a given time during the depolarization. The K^+ channels being virtually impermeant to Na^+ (Hille, 1973; Dubois & Bergman, 1975*a*), this experimental value is compared to the Nernst equilibrium potential, calculated as $E_K = RT/F$ (Log $[K]_o/[K]_i$) where $[K]_o$ and $[K]_i$ are the K^+ concentrations in the external bulk solution and in the internal solution bathing the cut ends of the fibre. This Nernst potential is referred to as the '*theoretical Nernst potential*'.

The potassium conductance (G_K) was calculated using:

$$G_K = I_K/(E-E_K), \tag{1}$$

where I_K is the potassium current; E is the membrane potential and E_K is either the actual equilibrium potential for K^+ ions or the theoretical Nernst potential.

Instantaneous reversal potential measurements

The tail of the K^+ current occurring at repolarization not only reflects the shutting off of the K^+ conductance but also the change in concentration of K^+ ions accumulated in the perinodal space during the pulse. Taking advantage of the analog compensation for both the capacity and the leakage currents, the reversal potential for the K^+ current at the end of a clamp pulse (the main pulse) was determined experimentally by changing the membrane potential during a second voltage clamp pulse (post pulse) until the initial part of the tail current reached the zero current level. The corresponding membrane potential was taken as the actual instantaneous reversal potential.

RESULTS

1. *Instantaneous reversal potential*

Fig. 1 shows K^+ current traces recorded either in 2·5 or 117 mM-K in response to different main and post pulse amplitudes. In 2·5 mM-K, the current tail occurring at the end of a main pulse which lasted 10 msec and took the membrane potential to $E = +40$ mV was recorded at various potentials between $E = -90$ mV and $E = -13$ mV during the post pulse (Fig. 1*B–F*). The initial value of the tail current is found to be nil at a potential (instantaneous reversal potential $= -38$ mV) more positive than the theoretical Nernst potential (-95 mV) (see definitions in Methods). The instantaneous reversal potential is regarded as the actual equilibrium potential for K^+ ions. Under similar experimental conditions, it has been found that the instantaneous reversal potential varies from one fibre to another (see Table 1). This variation may be due to the fact that the experiments were performed indiscriminately

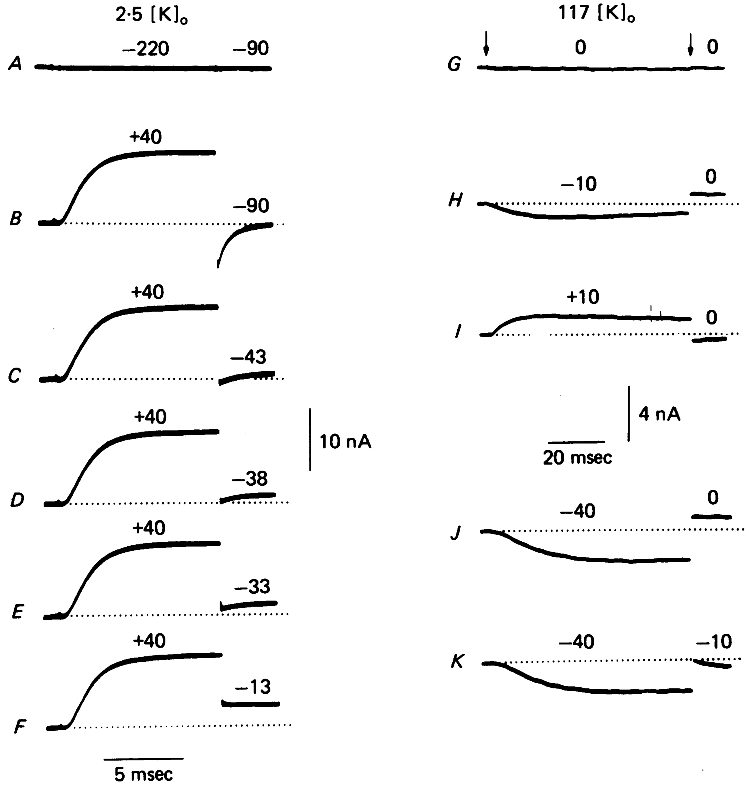

Fig. 1. Recordings of delayed and tail currents showing the change in E_K during a voltage pulse. The currents were recorded in 2·5 mM-K (left) (fibre: 27–4–7) and in 117 mM-K (right) (fibre: 4–2–7). Holding potential $= -90$ mV. *A*, in response to a hyperpolarizing pulse of 130 mV after correction for leakage and capacity currents: this record is presented to show the compensation accuracy. *B–F*, delayed currents recording during the same depolarizing pulse and tail currents recorded at different repolarizing levels (voltage indicated by numbers). −38 mV (*D*) is considered as the reversal potential for the instantaneous current. Theoretical Nernst potential $= -95$ mV. *G*, current recorded in 117 mM-K at $E = 0$ mV. The arrows indicate the beginning and the end of the main pulse. *H*, *I*, steady-state inward and outward currents followed by a tail current recorded at the theoretical Nernst Potential ($E = 0$ mV). *K*, tail current recorded at a potential (-10 mV), considered as the actual equilibrium potential for K^+ ions at the end of the inward delayed current. The dashed lines represent the zero current. Note that in *F*, the amplitude of the tail current is almost constant. This suggests a simultaneous decrease in G_K and increase in driving force resulting from a redistribution of K^+ ions accumulated into the perinodal space during the main pulse. In *D* and *K*, the voltage of the second pulse is considered as the reversal potential for the instantaneous current, the tail current becomes outward (*D*) or inward (*K*). The variation in amplitude of these tail currents is attributed to a change in driving force resulting from a rapid redistribution of K^+ ions.

on both motor and sensory fibres which are known to exhibit different amounts of K^+ accumulation (Neumcke, Schwarz & Stämpfli, 1980).

In 117 mM-K (Fig. 1*G–K*), the instantaneous reversal potential at the end of depolarizing pulses lasting 70 msec depends on both the intensity and the direction of the K^+ current elicited by the main pulse. When this current is inward, the instantaneous reversal potential is found to be more negative than the theoretical Nernst potential (Fig. 1*H–K*). When the K^+ current during the main pulse is outward, the instantaneous reversal potential is found to be positive (Fig. 1*I*). In 117 mM-K, it is much less shifted from the theoretical Nernst Potential than in 2·5 mM-K. The instantaneous reversal potential varies from one fibre to another and does not significantly differ from the theoretical Nernst potential for 40 % of the fibres (see Table 1).

TABLE 1. Instantaneous reversal potential (IRP) at the end of depolarizing pulses of duration t to a potential E, in 2·5 and 117 mM-K. Temperature: 12 °C. Holding potential: −90 mV

	2·5 mM-K		117 mM-K			
	$E = +20$ mV		$E = -40$ mV		$E = +20$ mV	
Fibre	IRP (mV)	t (msec)	IRP (mV)	t (msec)	IRP (mV)	t (msec)
5–1–7	−27	20	—	—	—	—
7–1–7	−49	20	—	—	—	—
21–12–7	−58	30	—	—	—	—
25–1–7	−62	30	—	—	—	—
27–1–7	−7	30	—	—	—	—
1–2–7	−14	30	—	—	—	—
4–2–7	−31	30	—	—	—	—
10–12–7	−34	30	—	—	—	—
2–12–7	+2	50	−3	50	+5	50
4–12–7	−38	50	0	50	0	50
10–3–7	—	—	−6	50	+7	50
20–4–7*a*	−31	50	−1	70	—	—
21–4–7	−44	50	−1	70	0	70
7–2–7	−16	70	—	—	+3	70
10–12–7	—	—	0	70	+2	70
26–4–7*a*	−23	70	−2	70	0	70
20–4–7*b*	—	—	−2	70	—	—
22–3–7	—	—	0	70	+5	70
26–4–7*b*	−20	70	0	70	+1	70
13–5–7	−20	70	−2	70	+1	70
17–5–7	−27	70	−1	70	+1	70
23–5–7	−45	70	0	70	0	70
11–2–7	−22	140	−6	140	+6	140

Variation of E_K with the voltage pulse amplitude

Assuming that the shift of E_K is produced by K^+ accumulation outside the membrane (Dubois & Bergman, 1975*b*; Attwell *et al.* 1980), one would expect that the actual value of E_K would depend on the size of the voltage pulse, since the corresponding current depends on the membrane potential. Therefore the steady-state K^+ currents were measured at the end of 140 msec depolarizing pulses of various amplitudes in 2·5 and 117 mM-K (Fig. 2*A* and *D*). For each depolarizing pulse, a set of tail current recordings was obtained by changing the post-pulse potential. The actual value of E_K (instantaneous reversal potential) was then determined using the procedure described in the methods. Fig. 2*B* and *E* show the variation of the instantaneous reversal potential as a function of the membrane polarization during the main pulse in 2·5 and 117 mM-K respectively. It can be seen that the variation of instantaneous reversal potential is more dramatic in 2·5 mM-K than in 117 mM-K. As expected from the transfer of ions from one side of the membrane to the other, the shift of the instantaneous reversal potential from the theoretical Nernst potential

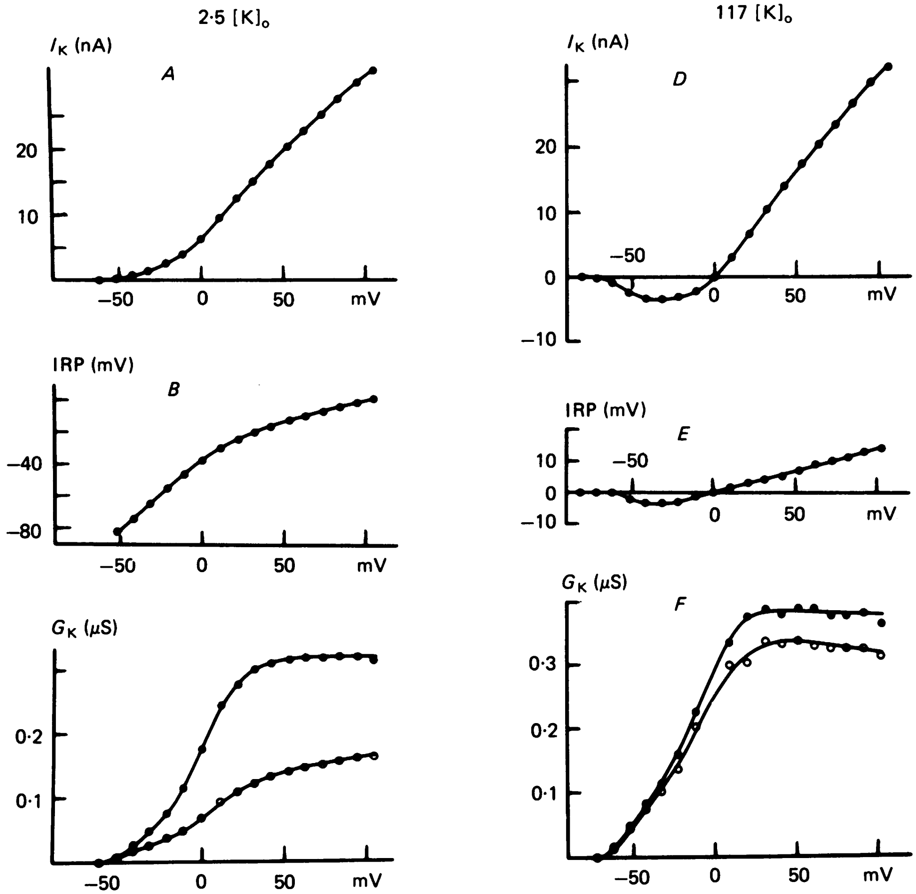

Fig. 2. Delayed current, reversal potential for the instantaneous K^+ current (IRP) and K^+ conductance as a function of membrane potential. The steady-state currents (*A* and *D*) and IRP (*B* and *E*) were recorded at the end of a 140 msec depolarizing pulse of various amplitudes in 2·5 mM-K (left) and 117 mM-K (right). The conductance (*C* and *F*) was calculated using eqn. (1) with the theoretical Nernst potential (○) or the actual E_K (IRP) (●). Note the simultaneous variation of I_K and IRP and the discrepancies between the G_K–E curves calculated with the theoretical and the actual E_K, Fibre: 11–2–7.

in 117 mM-K is negative when the steady-state K^+ current is inward and positive when the steady-state K^+ current is outward. In 2·5 mM-K, at the end of a depolarizing pulse to $E = +100$ mV, the instantaneous reversal potential is nearly equal to zero indicating that, under these conditions the external and internal concentrations are almost equal.

Since the instantaneous K^+ current–voltage relationships are linear in low and high K^+ media (Dubois & Bergman, 1977; Attwell *et al.* 1980), the conductance can be used as an expression of the permeability state of the membrane. For comparison, the K^+ conductance was calculated using either the theoretical E_K (-95 mV in 2·5 mM-K and 0 mV in 117 mM-K) or the actual values of E_K estimated at the end of the pulses. While the two conductance-potential curves are very similar for moderate depolarizations in 117 mM-K (Fig. 2*F*), marked differences are observed in 2·5 mM-K (Fig. 2*C*). In both K^+ solutions, the conductance (calculated using the actual E_K) tends to saturate for large depolarizations. When calculated using the theoretical E_K in 2·5 mM-K the conductance continues to increase with large depolarizations and no saturation is observed.

These results show that E_K depends on the size of the steady-state K^+ current elicited by a depolarization. For long lasting and large depolarizations in a low external K^+ concentration medium, the concentration gradient for K^+ ions is substantially reduced and tends to zero. When calculated using the actual E_K, the conductance tends to saturate for large depolarizations and the conductance-potential curve is noticeably different (especially in 2·5 mM-K) from the curve obtained using the theoretical E_K. One further useful piece of information can be obtained from the data in Fig. 2. The conductance voltage curves (as calculated using the actual E_K) are different in the two media (Fig. 2*C* and *F*). Moreover, the maximum conductance is higher in 117 mM-K than in 2·5 mM-K. These results are in agreement with the previous observations that the K^+ conductance not only depends on the membrane potential but also on the external K^+ concentration (Dubois & Bergman, 1977; Attwell *et al.* 1980).

Conductance turn on kinetics

The preceding results show that the electrochemical gradient for K^+ ions depends on the history of the magnitude and direction of the potassium current. This implies that the time course of the K^+ current reflects both the kinetics of the conductance change and the variation of E_K. Experiments were undertaken to describe the actual change in conductance after correction for the concomitant change in E_K.

Using G_K to describe the activation state of the K system, the kinetics of the K^+ conductance change in response to a sudden depolarization can be described in the framework of the Hodgkin–Huxley model by

$$G_K = [G_{K_\infty}{}^{1/a} - (G_{K_\infty}{}^{1/a} - G_{K_0}{}^{1/a})e^{-t/\tau}]^a, \qquad (2)$$

with G_{K_∞}: steady-state conductance during the depolarization; G_{K_0}: steady-state conductance before the depolarization; τ: time constant of the conductance change.

For a large negative holding potential, G_{K_0} is nearly zero and eqn. (2) can be written

$$G_K = G_{K_\infty}\,(1 - e^{t/\tau})^a. \qquad (2')$$

The following series of experiments was undertaken to determine whether eqn. (2′) satisfactorily describes the actual time course of G_K. Both the actual values of I_K and instantaneous reversal potential were measured at the end of test pulses of various durations and constant amplitudes in 2·5 and 117 mM-K-solutions. Then, the corresponding conductances were calculated using eqn. (1) (Fig. 3).

In 2·5 mM-K, a large depolarizing pulse ($E = +80$ mV) leads to a large change in

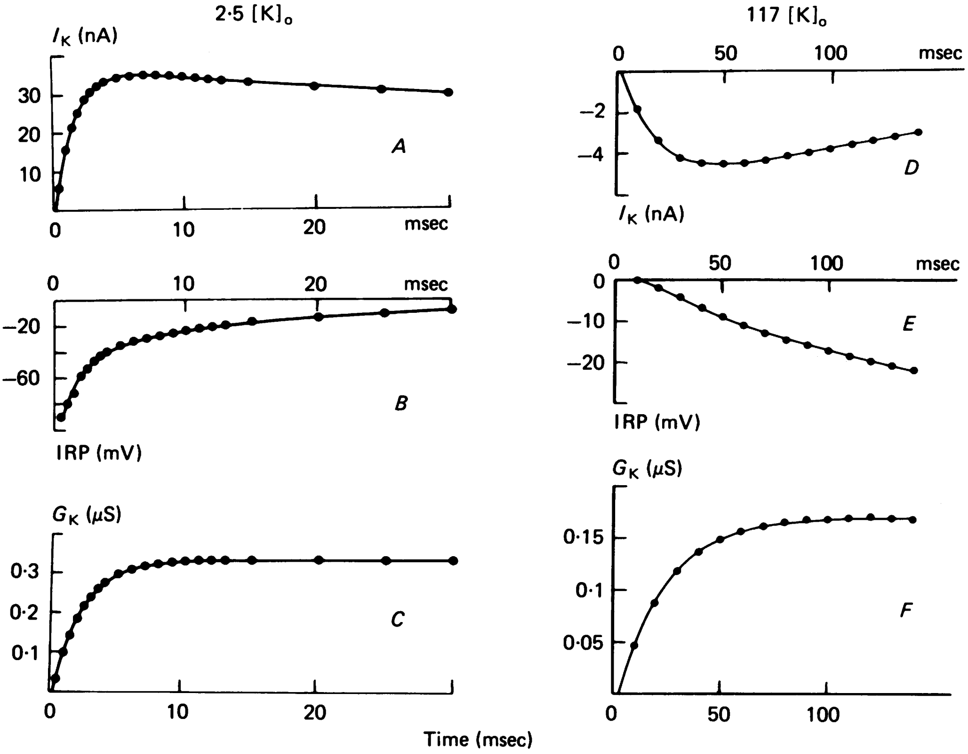

Fig. 3. Delayed current, reversal potential for the instantaneous K^+ current (IRP) and K^+ conductance as a function of time. The currents (*A* and *D*) and IRP (*B* and *E*) were recorded at the end of a depolarizing pulse of various durations in 2·5 mM-K (left) and 117 mM-K (right). The potential was +80 mV in 2·5 mM-K and −40 mV in 117 mM-K. The conductance (*C* and *F*) was calculated according to eqn. (1) with the actual E_K (IRP). The curves in *C* and *F* were calculated according to eqn. (3) assuming $\delta t = 0{\cdot}3$ msec (*C*) and 2·5 msec (*F*); $\tau = 2{\cdot}15$ msec (*C*) and 22·5 msec (*F*); $G_{K_\infty} = 0{\cdot}333\,\mu S$ (*C*) and $0{\cdot}166\,\mu S$ (*F*). Fibre: 4–2–7.

instantaneous reversal potential towards positive values which increases with the pulse duration.

In 117 mM-K, a depolarization taking the membrane potential to a lower value ($E = -40$ mV) than the steady-state reversal potential of I_K leads to a change in instantaneous reversal potential in the other direction. One can see (Fig. 3*A*) that the time course of the current noticeably differs from the kinetics of the conductance change (Fig. 3C). In particular, the rise in conductance is apparently slower than that of the current and while the conductance reaches a steady-state level, the current reaches a peak and then decreases. This late decrease of I_K appears similar to the fast inactivation of I_K described by Schwarz & Vogel (1971). The results of Fig. 3 suggest that this decrease in I_K is more likely due to a decrease in driving force than to G_K inactivation. This point will be discussed in the following paper (Dubois, 1981).

To determine the value of the exponent a, in eqn. (2′), $1-(G_K/G_{K_\infty})^{1/a}$ has been plotted versus time on a semilogarithmic scale and the value of a was changed until the points could be fitted by a straight line (Fig. 4*A*). Using this procedure for twelve fibres, only one value ($a = 1$) could satisfactorily produce a straight line in 2·5 and 117 mM-K.

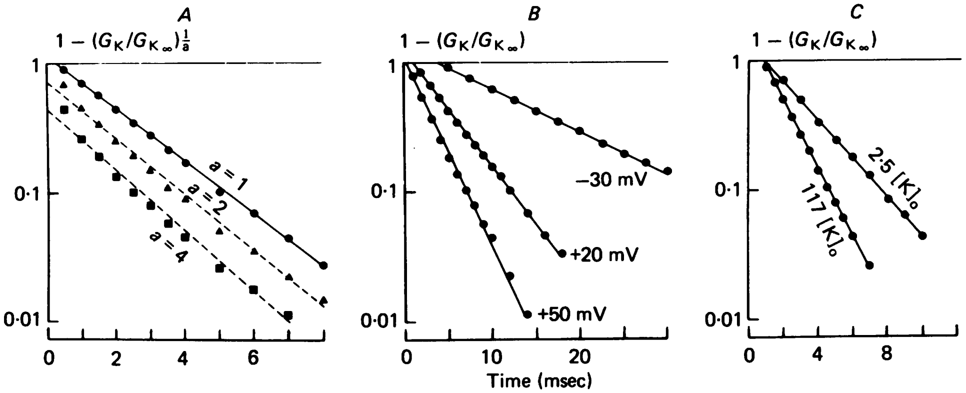

Fig. 4. Semilogarithmic plots of G_K activation. The conductance was calculated and plotted versus time according to eqn. (2′): $\log[1-(G_K/G_{K\infty})^{1/a}] = -t/\tau$. In *A*, G_K was calculated from current recordings in 2·5 mM-K at $E = +80$ mV. Different values (1, 2, 4) for the exponent a were used. The straight lines (continuous for $a = 1$, interrupted for $a = 2$ and 4) were obtained by least-squares fitting to the points. The best fit is obtained with $a = 1$. The delay (δt) is the time lag at the onset of the depolarization. It is obtained from the (extrapolated) intercept of the straight line with the upper horizontal axis at ordinate value 1. Fibre: 4–2–7. In *B*, the conductance was calculated in 117 mM-K at different membrane potentials. $a = 1$. The three sets of points are distributed along straight lines. The time constant and the delay decrease with increasing depolarization. Fibre; 20–4–7. In *C*, the conductance was calculated at $E = +20$ mV in 2·5 mM-K and 117 mM-K. $a = 1$. In the two media, the delay is the same, the time constants are different, larger in 2·5 mM-K than in 117 mM-K. Fibre: 17–5–7.

With this value of a the extrapolated straight line intercepts the ordinate at a value greater than 1, implying that a delay (δt) must be introduced in eqn. (2′) as already proposed for the sodium system of the squid axon (Armstrong & Bezanilla, 1974; Keynes & Rojas, 1976) and the Ranvier node (Neumcke, Nonner & Stämpfli, 1976). Accordingly, eqn. (2′) must be replaced by

$$G_K = G_{K_\infty}\,[1-\exp\{-(t-\delta t)/\tau\}] \qquad (3)$$

With increasing depolarizations, the delay δt decreases and the slope of the straight line increases (i.e. τ decreases) (Figs. 4*B* and 5).

The above analyses could be in error if in fact G_{K_0} does not equal zero. An upper limit of G_{K_0} can be estimated from Fig. 6*B*. Assuming that leakage current is linear and outward gating current is nil after 1 msec of depolarization, G_{K_0} must be less than $0{\cdot}019\bar{G}_K$. However, even this value of G_{K_0} is introduced into eqn. (2), the data of Fig. 4*A* remain better fitted by eqn. (3) than by eqn. (2) with $a = 2$ or 4.

It was of interest to know whether, at constant membrane potential, the value of τ was affected by changes in the external K^+ concentration. The K^+ conductance was calculated for the same fibre at $E = +20$ mV in 2·5 and 117 mM-K and the time constants of activation were deduced from analyses of the change in conductance at this potential. In 117 mM-K, the instantaneous reversal potential was found to be constant during the depolarization, thus the kinetics of the current change reflected faithfully the kinetics of the conductance change. In 2·5 mM-K, the conductance was calculated from I_K and instantaneous reversal potential measurements.

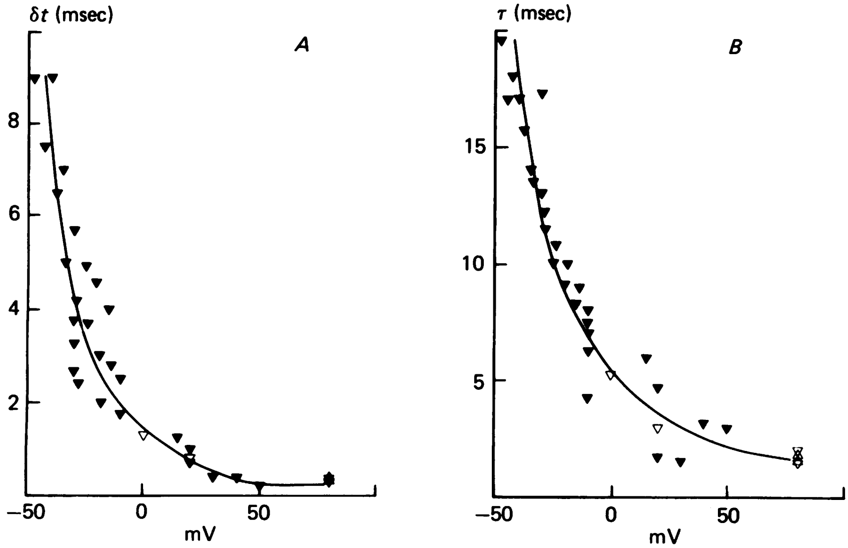

Fig. 5. Delay (*A*) and time constant (*B*) of the K^+ conductance activation versus membrane potential during the test depolarization. The delay (δt) and the activation time constant (τ) were calculated according to eqn. (3) in 117 mM-K (filled symbols) and 2·5 mM-K (open symbols) in different fibres. Temperature: 12 °C. Holding potential: −90 mV.

Fig. 4*C* shows that if the two sets of points are fitted by straight lines, the time constants are different (3 msec and 1·65 msec in 2·5 and 117 mM-K respectively). In four similar experiments, the ratio τ (2·5 mM-K)/τ (117 mM-K) was found to be: 1·21; 1·65; 1·75; 1·76. It thus appears that the time course of the increase in K^+ conductance is slower in 2·5 than in 117 mM-K, which agrees with the observations of Begenisich (1979).

Delayed turn on of the conductance; effect of hyperpolarizing prepulse

The results reported in the preceding section suggest that, at the onset of a depolarization, the K^+ conductance increase starts after a delay (δt). To prove the existence of this delay, the K^+ current was recorded in 117 mM-K at a membrane potential for which the change in instantaneous reversal potential was small in particular fibres. In such cases, the time course of the current is not influenced by accumulation. It should therefore mainly reflect the time course of the gating activation and can be described by

$$I_K = I_{K\infty}\,[1-\exp\{-(t-\delta t)/\tau\}]. \tag{4}$$

The K^+ current was recorded at $E = -20$ mV in 117 mM-K (Fig. 6*A*) and both parameters τ and δt in eqn. (4) were calculated. Then, at the same potential, the onset of the current was studied at high resolution after averaging the current responses to ten depolarizing and symmetrical hyperpolarizing voltage pulses (Fig. 6*B*). This procedure reduced the noise and any residual imperfectly compensated symmetrical capacity current. After a small transient of outward current, mainly reflecting the displacement of gating particles of the Na^+ channels (Nonner, Rojas & Stämpfli, 1975), a clear delay was observed before the onset of the inward K^+ current. This delay could not result from a superposition of an outward gating current and the inward K^+ current, because the time constant of the gating current is about 100 μsec at this potential (Nonner *et al.* 1975). The curve calculated using eqn. (4) and the parameters τ and δt obtained from the data of Fig. 6*A* satisfactorily fits the experimental recording. Thus, at least when no detectable change in the driving force occurs during the depolarization, the time course of the K^+ conductance activation can be described by a single exponential function provided a time lag is introduced.

In the squid giant axon, Cole & Moore (1960) reported that a delay in the K^+ current activation was induced by increasing the holding potential. In the Ranvier node. Palti *et al.* (1976) also observed a change in the kinetics of the K^+ current activation on increasing the magnitude of a hyperpolarizing prepulse. Recently, Begenisich (1979) has made a quantitative study of the delayed activation of the K^+ current in the Ranvier node from northern *R. pipiens*. In this preparation, the K^+ currents produce little accumulation of K^+ ions outside the membrane (Armstrong & Hille, 1972; Begenisich, 1979). Thus, it is assumed that the kinetics of the current change recorded in normal K^+ Ringer reflects faithfully the kinetics of the conductance activation. Begenisich concluded that hyperpolarizing prepulses increase the delay and modify the activation kinetics of the K^+ current. Taking account of this observation, it was of interest to known whether, with a hyperpolarizing prepulse, the activation of the K^+ conductance can still be described by eqn. (3) and whether or not the time constant of activation is changed by the prepulse.

The current was recorded in K-rich media during depolarizing pulses following a 55 msec prepulse of various amplitudes. For this purpose, fibres in which no noticeable change in instantaneous reversal potential could be observed in K-rich media were selected. Fig. 6*C* presents a semilogarithmic plot of the K^+ current activation using eqn. (4). The current was recorded during a depolarization to $E = -40$ mV with or without a 30 mV hyperpolarizing prepulse. The two sets of points fall along two parallel straight lines, thus implying a simple shift of the current by 1·4 msec. However, especially with the negative prepulse, a clear deviation of the experimental points from the straight line is observed during the first few milliseconds. This observation implies that the single exponential function with a delay (eqn. (3)) should only be regarded as a convenient expression to describe the time course of the

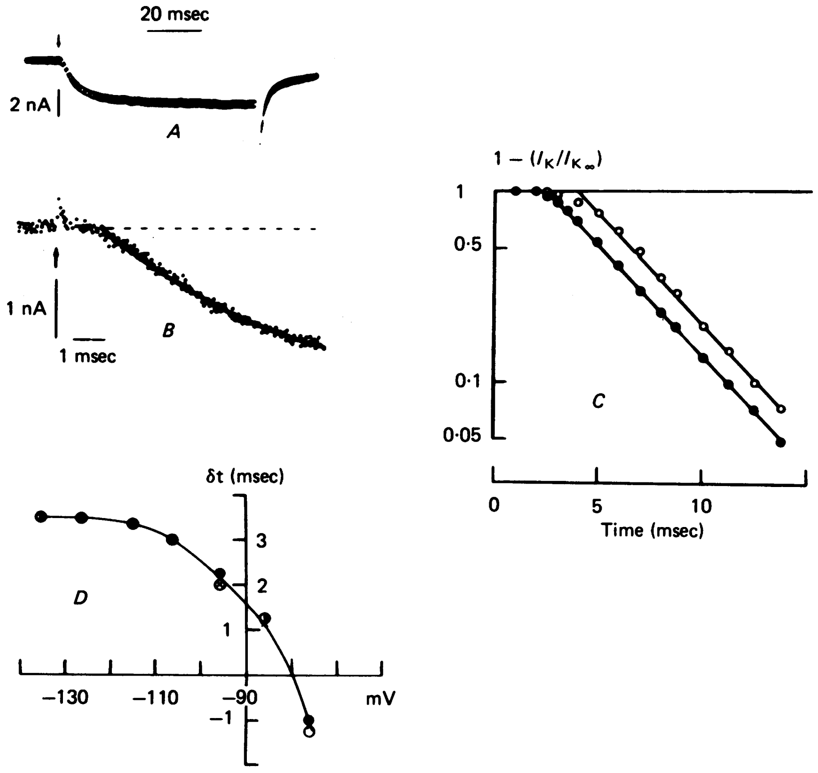

Fig. 6. Delayed activation of the conductance. The inward current was recorded from fibres in which no change in instantaneous reversal potential could be observed in K-rich media thus the current is assumed to be directly proportional to the conductance.

A and *B*: the current was recorded on the same fibre during a depolarization of 70 mV ($E = -20$ mV) from a holding potential of −90 mV in 117 mM-K. Fibre: 17–5–7. *A*: single sweep trace if I_K. The white points represent the theoretical current as calculated using eqn. (4) with $\delta t = 1{\cdot}3$ msec, $\tau = 6{\cdot}3$ msec, $I_{K\infty} = 3$ nA. The arrow indicates the beginning of the depolarization. *B*: averaged onset of the current in response to ten 70 mV depolarizing and hyperpolarizing pulses ($E = -20$ mV and −160 mV). The curve represents the theoretical current as calculated using the same equation and the same parameters as in *A*. Note the time lag at the onset of the depolarization between the small outward displacement current and the beginning of the inward K$^+$ current.

C: the current, recorded in 117 mM-K at $E = -40$ mV, from a holding potential of −90 mV without (●), and with (○), a 55 msec prepulse to $E = -120$ mV, is plotted *vs.* time according to eqn. (4) log $(1 - I_K/I_{K\infty}) = -t/\tau$. Note the translation of the straight line with the hyperpolarizing prepulse and the deviation of the experimental points from the straight lines in the first milliseconds. Fibre: 8–6–7.

D: the current was recorded in 117 mM-K (●), 60 mM-K (○) and again in 117 mM-K (crosses) at $E = -30$ mV with a 55 msec prepulse of various amplitudes. The delay deduced from graphs similar to that of *C* is plotted versus prepulse potential. Note that the delay, independent of $[K]_0$, increases with prehyperpolarization and saturates near −120 mV. For prepulses less negative than −80 mV, the delay is found to be negative. This is due to the fact that, under these conditions, the conductance is partially activated at the end of the prepulse. Fibre: 11–7–8.

conductance change. In Fig. 6*D*, the delay, plotted against the voltage during the prepulse, was calculated in 117 and 60 mM-K solutions using eqn. (4). It can be seen that the delay is independent of the extenal K^+ concentration, thus confirming the result of Fig. 4*C*. The delay increases with the hyperpolarization during the prepulse to reach a steady-state level below -120 mV.

Turning off of the conductance

After a conditioning depolarization activating the K^+ conductance, a tail of inward current is recorded at the holding potential. In the 2·5 mM-K solution, the time course of this current reflects both the kinetics of channels closing and the variation of E_K. The actual values of E_K (instantaneous reversal potential) during the turning off of the tail current can be determined as described in the methods using a second pulse starting at a different time after the end of the conditioning depolarization. The kinetics of the shutting off of the conductance can be calculated from the values of the current measured at different times after the end of the conditioning depolarization and the corresponding values of instantaneous reversal potential. In the 117 mM-K solution and under conditions in which no change in E_K can be expected during the conditioning depolarization, the kinetics of the tail current should reflect the kinetics of the turning off of the conductance if the tail current does not itself induce a change in E_K. The following series of experiments was undertaken to determine (i) the kinetics of the turning off of the conductance in low and high K^+ solutions, and (ii) in the low K^+ solution, the time course of the variation of E_K reflecting the restoration of the initial K^+ concentration in the perinodal space.

The tail current was recorded in 117 mM-K at $E = -100$ mV after a conditioning depolarization of 100 msec to $E = 0$ (Fig. 7*A*). Then, during the development of the tail current and at various times after the end of the conditioning depolarization, the membrane was repolarized to $E = 0$ (the potential value which corresponds to theoretical Nernst potential (Fig. 7*B*). During the second depolarization, the current is nil whatever the duration of the transient repolarization. This result implies that under the experiment conditions, E_K is constant during the tail current in 117 mM-K, and consequently the kinetics of the tail current change reflect faithfully the kinetics of the conductance change. It must be noted that in 117 mM-K and after a conditioning pulse to 0 mV, E_K was generally found to be constant during the development of the tail current, even in fibres exhibiting a noticeable change in E_K during depolarizations to membrane potentials different than 0 mV.

In 2·5 mM-K, the tail current at $E = -100$ mV (Fig. 7*C*) and instantaneous reversal potential values during the development of this tail current (Fig. 7*D*) were recorded after a depolarization of 100 msec to 0 mV. From the variation of this potential, one can deduce that the restoration of the initial K^+ concentration is almost complete within 8 msec and is concomitant with the change in current.

The conductance, normalized to its value at the end of the conditioning pulse, was calculated in 2·5 and 117 mM-K from the data of Fig. 7*A*, *C* and *D* (Fig. 7*E*). Three results were found which are not predicted by the H–H model: (i) the kinetics of the shutting off of the conductance is slower in 117 than in 2·5 mM-K; (ii) in both solutions, the kinetics of the conductance change cannot be described by a single exponential function; (iii) after a fast declining phase, the conductance decreases very slowly for several hundred milliseconds (partially represented in the Figure).

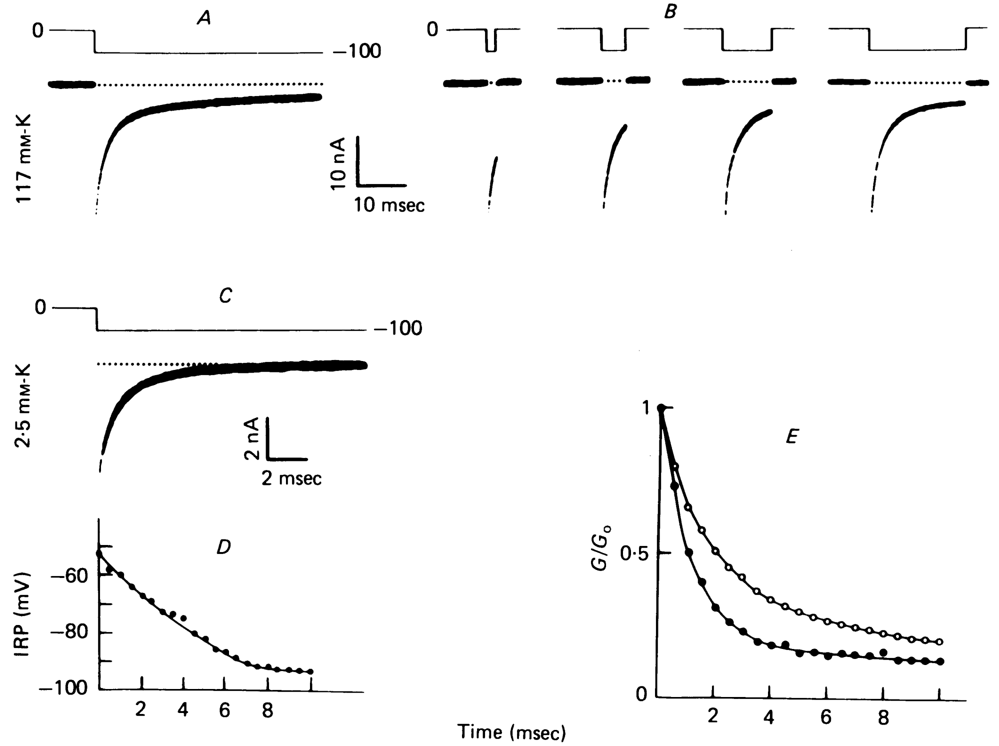

Fig. 7. Kinetics of turning off of the conductance. The tail current was recorded in 117 mM-K (*A* and *B*) and 2·5 mM-K (*C*) at $E = -100$ mV after activation of the conductance by a 100 msec depolarizing pulse to $E = 0$ mV (conditioning pulse). In 117 mM-K, the potential during the conditioning pulse corresponds to theoretical Nernst potential, the current is nil (*A*) and no change in E_K can be suspected. In *B*, the membrane was repolarized to $E = 0$ mV respectively 2, 5, 10 and 20 msec (from left to right respectively) after the end of the conditioning pulse. The current is nil during the second depolarization. This indicates that at repolarization the large influx of K^+ ions does not induce noticeable change in E_K. Consequently, the time course of the tail current reflects faithfully the kinetics of the conductance change. In 2·5 mM-K, a second pulse of variable amplitude was applied at different time during the development of the tail current. From the initial values of the current recorded during the second pulse, the instantaneous reversal potential was evaluated every 500 μsec after the end of the conditioning pulse (D). The conductance normalized to its value at the end of the conditioning pulse was calculated in 117 (○) and 2·5 mM-K (●) from the data of *A*, *C* and *D* (*E*). The slow decrease in conductance is faster in 2·5 than in 117 mM-K. The interrupted line denotes the zero current level. Fibre: 6–3–9.

In 2·5 mM-K, it must be noted that after 10 msec of repolarization the tail current is almost nil whereas the conductance remains relatively large (10 % of its initial value) (see also Bergman, Dubois & Bergman, 1980). This is due to the fact that the restoration of the K^+ concentration into the perinodal space is faster than the change in conductance. After 10 msec of repolarization to -100 mV, the electrochemical gradient for K^+ ions and consequently the current are almost nil.

DISCUSSION

The present results show that, during a depolarization, the equilibrium potential for K^+ ions, defined as the reversal potential for the instantaneous K^+ current, changes continuously and depends on both the direction and the intensity of the delayed current. When the latter is outward, the change in E_K can be explained as resulting from an accumulation of K^+ ions in the perinodal space (Armstrong & Hille, 1972; Dubois & Bergman, 1975*b*; Ochs & Bromm, 1976; Attwell *et al.* 1980). When the K^+ current is inward (in a K-rich medium), the change of E_K can be due to a depletion of K^+ from the perinodal space.

In previous works (Dubois & Bergman, 1977; Attwell *et al.* 1980) it has been shown that the steady-state K^+ conductance was found to depend upon the K^+ concentration in the external medium. This conclusion is confirmed by the present analysis.

At variance with earlier studies (Dodge, 1963; Frankenhaeuser, 1963; Koppenhöfer, 1967; Hille, 1968), the kinetic analysis presented here (Figs. 3, 4 and 6) shows that a single exponential function satisfactorily accounts for the time course of the conductance activation provided a 'delay' is interposed between the onset of the depolarization and that of the conductance change. This delay is defined as the time lag between the onset of the depolarization and the origin of the exponential function fitting most of the conductance change. The existence of a delay supports the two step model recently proposed by Dubois & Bergman (1977) and in some respects by Palti *et al.* (1976) to describe the activation of the K^+ permeability.

At repolarization, the kinetics of the turning off of the conductance cannot be described by a single exponential function. This observation, first reported by Frankenhaeuser (1963), is in agreement with a multi-step model since such a model predicts a multi-exponential decline of the conductance. However, a tentative decomposition into several exponential functions shows that the sum of (at least) three exponentials is necessary to describe the kinetics of the turning off of the conductance. In the framework of the multistep model proposed above, this would suggest that the turning off of the conductance proceeds in three transitions. An alternative interpretation (which is not incompatible with a multi-step model) is that the population of K^+ channels is not uniform and there are, within the membrane, several types of K^+ channels with different closing time constants. This hypothesis, already proposed by several authors (Schwarz & Vogel, 1971; Palti *et al.* 1976; Van den Berg, Siebenga & De Bruin, 1977; Ilyin, Katina, Lonskii, Makovsky & Polishchuk, 1977; Krylov & Makovsky, 1978) is further investigated in the following paper (Dubois, 1981).

The last point which deserves attention is the observation that the time constant of the conductance increase is larger in 2·5 mM-K than in 117 mM-K. This observation is consistent with the model proposed by Dubois & Bergman (1977) in which it was assumed that the opening of K^+ channels is triggered by K^+ ions. Independent of any possible effects of K^+ ions on channel gating, the increase in conductance, in 2·5 mM-K, should not only reflect time and voltage dependent gating but also the $[K]_o$ dependent conductance increase due to K^+ accumulation. In consequence, the over-all conductance should be described by

$$G_K = x_\infty \, \overline{G}_K \, [1 - e^{-(t-\delta t)/\tau}],$$

where x_∞ is the steady-state gating activation parameter and $\overline{G}_K$ the maximum conductance (function of $[K]_0$). Under these conditions, it appears that, in 2·5 mM-K, the conductance increase should not be expected to be exponential since $\overline{G}_K$ should change with time. This conclusion does not agree with the results of Fig. 4*A* and *C*. One explanation is that the exponential increase in conductance (in 2·5 mM-K) is purely a coincidence. To test this interpretation, the variation of $\overline{G}_K$ with time should be calculated from the values of $[K]_0$ deduced from the instantaneous reversal potential. However, this verification requires knowledge of the relation between $\overline{G}_K$ and $[K]_0$. It will be shown in the following paper that the K^+ conductance is composed of several components whose K^+ dependences are different. This seriously complicates the analysis which can only be made on uniform conductance components.

From a practical point of view, the results show that any conductance analysis should be performed in absence of noticeable changes in E_K (K-rich media) or after correction for K^+ accumulation and not only for changes in driving force but also for changes in conductance related to variations in K^+ concentrations around the membrane.

I am grateful to C. Bergman for helpful suggestions and criticism throughout this work and to D. Attwell and S. Siegelbaum for critical reading of the manuscript.

REFERENCES

ADELMAN, W. J., PALTI, Y. & SENFT, J. P. (1973). Potassium ion accumulation in a periaxonal space and its effects on the measurements of membrane potassium ion conductance. *J. Membrane Biol.* **13**, 387–410.

ARMSTRONG, C. M. & BEZANILLA, F. (1974). Charge movement associated with the opening and closing of the activation gates of the Na channels. *J. gen. Physiol.* **63**, 533–552.

ARMSTRONG, C. M. & HILLE, B. (1972). The inner quaternary ammonium ion receptor in potassium channels of the node of Ranvier, *J. gen. Physiol.* **59**, 388–400.

ATTWELL, D., DUBOIS, J. M. & OJEDA, C. (1980). Fully activated potassium current-voltage relationship in the Ranvier node. *Pflügers Arch.* **384**, 49–56.

BEGENISICH, T. (1979). Conditioning hyperpolarization-induced delays in the potassium channels of myelinated nerve. *Biophys. J.* **27**, 257–266.

BERGMAN, J., DUBOIS, J. M. & BERGMAN, C. (1980). Post-tetanic membrane potentials in single axon and myelinated nerve trunk. *Ann. N.Y. Acad. Sci.* **339**, 21–38.

COLE, K. S. & MOORE, J. W. (1960). Potassium ion current in the squid giant axon: dynamic characteristic. *Biophys. J.* **1**, 1–14.

DODGE, F. A. (1963). A study of ionic permeability changes underlying excitation in myelinated nerve fibres of the frog. Thesis, The Rockefeller University. University Microfilms, Inc., Ann Arbor (no. 64–7333).

DUBOIS, J. M. (1981). Evidence for the existence of three types of potassium channels in the frog Ranvier node membrane. *J. Physiol.* **318**, 297–316.

DUBOIS, J. M. & BERGMAN, C. (1975*a*). Late sodium current in the node of Ranvier. *Pflügers Arch.* **357**, 145–148.

DUBOIS, J. M. & BERGMAN, C. (1975*b*). Potassium accumulation in the perinodal space of the frog myelinated axons. *Pflügers Arch.* **358**, 111–124.

DUBOIS, J. M. & BERGMAN, C. (1977). The steady-state potassium conductance of the Ranvier node at various external K-concentrations. *Pflügers Arch.* **370**, 185–194.

FRANKENHAEUSER, B. (1962). Potassium permeability in myelinated nerve fibres of *Xenopus laevis*. *J. Physiol.* **160**, 54–61.

FRANKENHAEUSER, B. (1963). A quantitative description of potassium currents in myelinated nerve fibres of *Xenopus laevis*. *J. Physiol.* **169**, 424–430.

Frankenhaeuser, B. & Hodgkin, A. L. (1956). The after-effects of impulses in the giant nerve fibres of *Loligo*. *J. Physiol.* **131**, 341–376.

Ganot, G., Palti, Y. & Stämpfli, R. (1978). Cole–Moore effect in the frog node. *Proc. natn. Acad. Sci. U.S.A.* **75**, 3254–3257.

Goldman, D. E. (1943). Potential, impendence and rectification in membrane. *J. gen. Physiol.* **27**, 37–60.

Hille, B. (1968). Charges and potentials at the nerve surface: Divalent ions and pH. *J. gen. Physiol.* **51**, 221–236.

Hille, B. (1973). Potassium channels in myelinated nerve. *J. gen. Physiol.* **61**, 669–686.

Hodgkin, A. L. & Katz, B. (1949). The effect of sodium ions on the electrical activity of the giant axon of the squid. *J. Physiol.* **108**, 37–77.

Ilyin, V. I., Katina, I. E., Lonskii, A. V., Makovsky, V. S. & Polishchuk, E. V. (1977). Evidence of the existence of the two independent components of potassium current in the Ranvier node of the frog *Rana ridibunda*. *Dokl. Akad. Nauk SSSR.* **234**, 1467–1470.

Keynes, R. D. & Rojas, E. (1976), The temporal and steady-state relationship between activation of the sodium conductance and movements of the gating particles in the squid giant axon. *J. Physiol.* **255**, 157–189.

Koppenhöfer, E. (1967). Die Wirkung von Tetraäthylammonium chloride auf die Membranströme Ranvierscher Schnürringe von *Xenopus laevis*. *Pflügers Arch.* **293**, 34–55.

Krylov, V. V. & Makovsky, V. S. (1978). Spike frequency adaptation in amphibian sensory fibres is probably due to slow K-channels. *Nature, Lond.* **275**, 549–551.

Neumcke, B., Nonner, W. & Stämpfli, R. (1976). Asymmetrical displacement current and its relation with the activation of sodium current in the membrane of frog myelinated nerve. *Pflügers Arch.* **363**, 193–203.

Neumcke, B., Schwarz, W. & Stämpfli, R. (1980). Differences between K channels in motor and sensory nerve fibres of the frog as revealed by fluctuation analysis. *Pflügers Arch.* **387**, 9–16.

Nonner, W. (1969). A new voltage clamp method for Ranvier nodes. *Pflügers Arch.* **309**, 116–192.

Nonner, W. Rojas, E. & Stämpfli, R. (1975). Displacement currents in the node of Ranvier. *Pflügers Arch.* **354**, 1–18.

Ochs, G. & Bromm, B. (1976). P current and K^+ accumulation in the perinodal space; effects on the action potential. *Pflügers Arch.* (suppl.) **365**, R34.

Palti, Y., Ganot, G. & Stämpfli, R. (1976). Effect of conditioning potential on potassium current kinetics in the fog node. *Biophys. J.* **16**, 262–273.

Palti, Y., Gold, R. & Stämpfli, R. (1979). Diffusion of ions in myelinated nerve fibers. *Biophys. J.* **25**, 17–31.

Schwarz, J. R. & Vogel, W. (1971). Potassium inactivation in single myelinated nerve fibres of *Xenopus laevis*. *Pflügers Arch.* **330**, 61–73.

Van den Berg, R. J., Siebenga, E. & De Bruin, G. (1977). Potassium ion noise currents and inactivation in voltage-clamped node of Ranvier. *Nature, Lond.* **265**, 177–179.